Supplemental Information

The Determination of the Location of Contact Electrification-Induced Discharge Events

Sarah J. Vella[a], Xin Chen[a], Samuel W. Thomas III[a], Xuanhe Zhao[b], Zhigang Suo[b], and George M. Whitesides*[a,c]

[a]*Department of Chemistry and Chemical Biology, Harvard University*

Cambridge, MA 02138

[b]*School of Engineering and Applied Sciences, Harvard University,*

Cambridge, MA 02138

[c]*Wyss Institute for Biologically Inspired Engineering, Harvard University,*

Cambridge, MA 02138

Charge on the sphere could induce charge in the magnet because it is conductive. The induced charge on the magnet, however, would not significantly affect the induced charge on the electrode because the electrode is located between the sphere and the magnet. On the other hand, there is no measurable induced current on the electrode or the sphere caused by the rotating magnet. The signal measured by the electrode as the magnet was spinning at 1000 rpm without a sphere, or with a stationary sphere (glued to the surface with epoxy) over the electrode, was no different from the random noise (< 5 pC) measured by the electrode when the magnet was not spinning (Figure S1).

Figure S1 – 60 s of data from a) the random noise measured by the electrode with the magnet not spinning; b) the signal measured by the electrode (w = 1 cm) with the magnet spinning at 1000 rpm; and c) the signal measured by the electrode with a stationary steel sphere (d = 3.2 mm) over the electrode (glued to the surface with epoxy) and the magnet spinning at 1000 rpm.

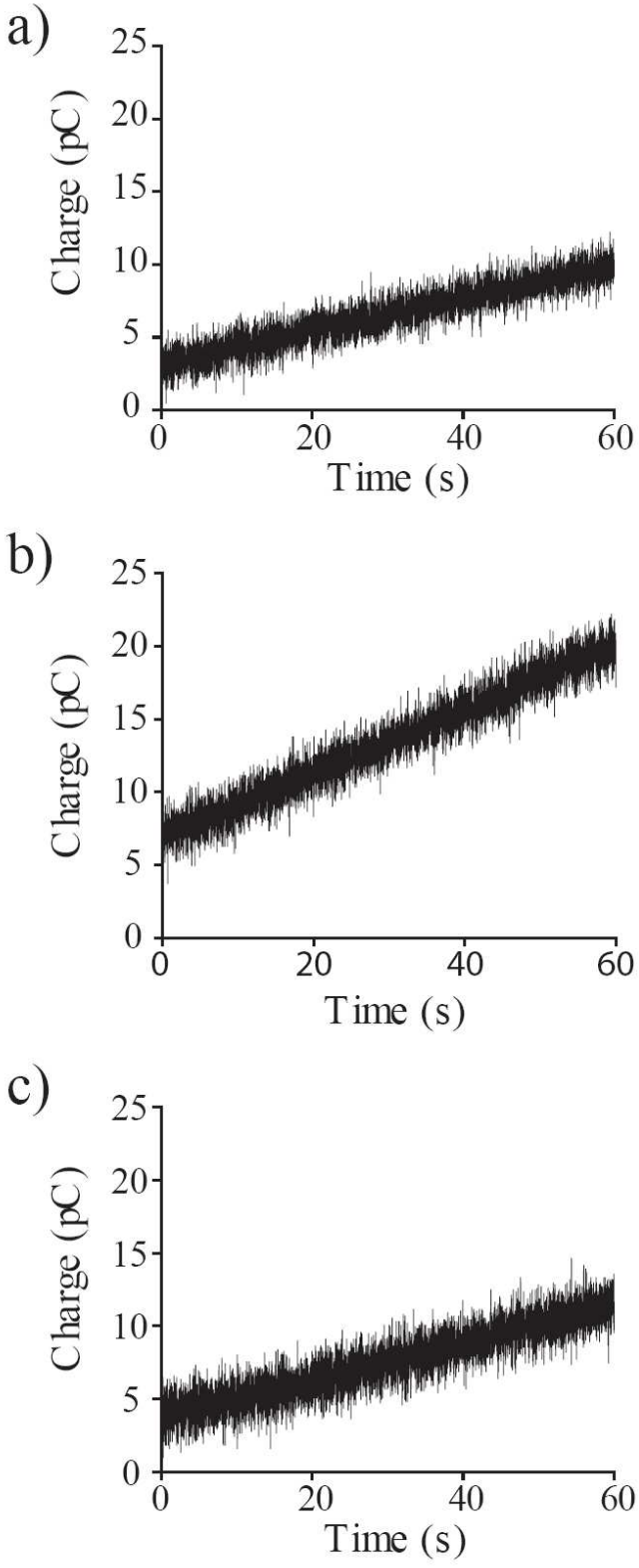
a)
Charge (pC)
25
20
15
10
5
0
0
20
40
60
Time (s)
b)
Charge (pC)
25
20
15
10
5
0
0
20
40
60
Time (s)
c)
Charge (pC)
25
20
15
10
5
0
0
20
40
60
Time (s)

Figure S2 – The electric potential gradient from the surface of the sphere a) with an electrode and b) without an electrode.

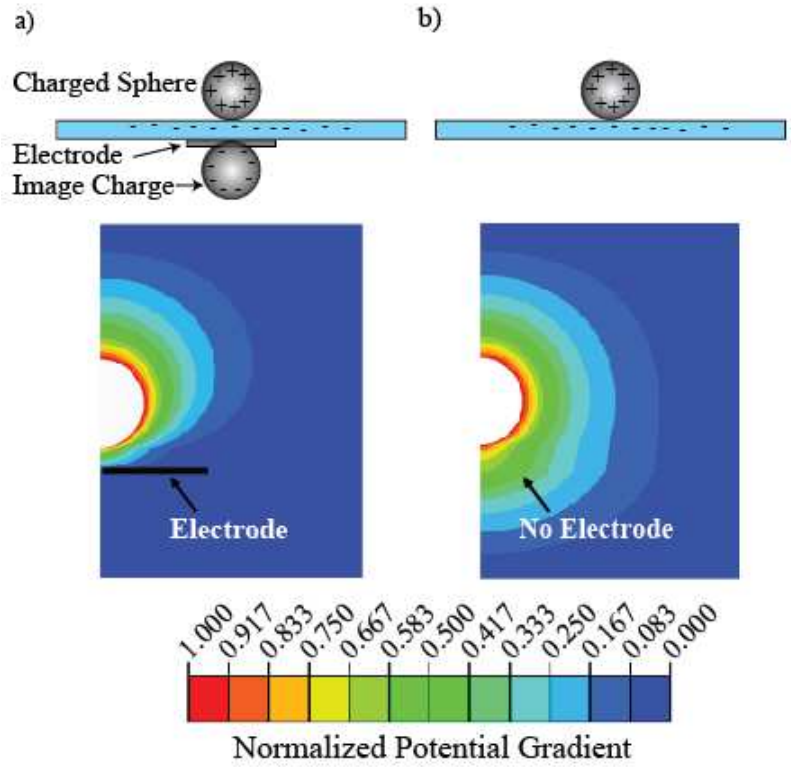

Using an axisymmetric model, the finite element software ABAQUS calculated the electric potential distribution around a charged sphere on a substrate; the relative dielectric constant for air was 1, and for the polymer substrate was 4. The electric potential gradient (i.e. electric field) below the charged ball was much higher with a grounded electrode beneath the substrate (Figure S1a), than without an electrode (Figure S1b). This larger electric field increased the probability of discharge when the sphere was above or close to the electrode.

Figure S3 – A steel sphere (d = 3.2 mm) rolling on a PS Petri dish (T ~ 25°C, RH < 10%): a) before plasma oxidation; b) after plasma oxidation of Zone **B** (as shown in Scheme 1) – 15 of the 25 discharges *shown* occurred in Zone **B**; c) an expanded view of the highlighted data in the blue box in (b) showing that the discharge was a "Peak" followed by "Baseline" disruption indicative of a Zone **B** discharge; d) after plasma oxidation of Zone **O** – 22 of the 22 discharges *shown* occurred in Zone **O** e) after plasma oxidation of Zone **A** – 16 of the 20 discharges *shown* occurred in Zone **A** (green arrows); f) an expanded view of the highlighted data in the blue box in (e) showing that the discharge is a "Baseline" followed by a "Peak" disruption indicative of a Zone **A** discharge.

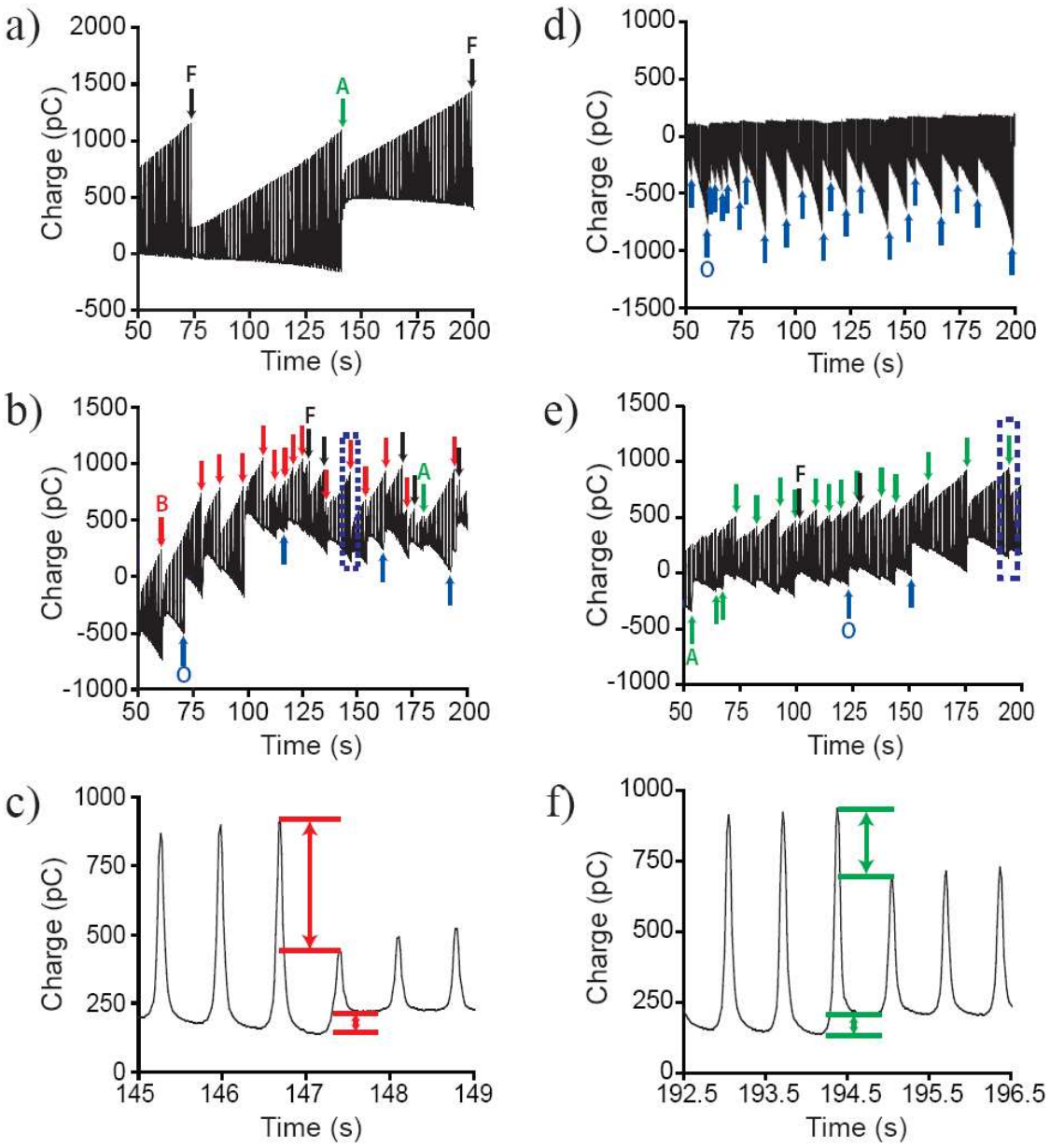
a)
Charge (pC)
Time (s)
F
A
F
b)
Charge (pC)
Time (s)
B
F
A
O
c)
Charge (pC)
Time (s)
d)
Charge (pC)
Time (s)
O
e)
Charge (pC)
Time (s)
F
A
O
f)
Charge (pC)
Time (s)

For samples that only had a region plasma oxidized, the charging occurred almost entirely when the sphere rolled on the oxidized region of the PS dish. Figure S3 shows data from a steel sphere rolling on a plasma-oxidized PS Petri dish where the oxidized zone was positioned over the electrode (Zone **O**); both the steep slope of the baseline (Q_{dne}), and the lack of increase in $\{Q_s + Q_{dne}\}$, indicated that charge separation occurred almost exclusively over Zone **O**. Although this charging trend was not as apparent in the data traces from a steel sphere rolling on a PS dish in which only Zone **B**, or Zone **A**, had been plasma oxidized, we assumed that charge separation also occurred more rapidly over the treated regions. The unequal charging rate over the surface must also result in more charge on the treated region than the untreated region.

Figure S4 – 25s of data from a steel sphere (d = 3.2 mm) rolling on a Zone O plasma-oxidized PS Petri dish. Both the steep slope of the baseline (Q_{dne}, □ • •) and the lack of increase in $\{Q_s + Q_{dne}\}$ (□ □ □) indicate that charge separation occurred almost exclusively over Zone O.

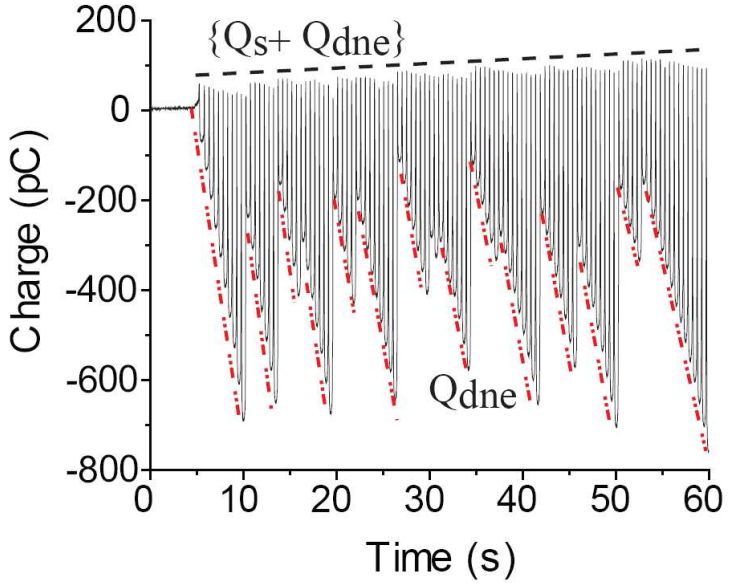

Derivation of Eq. 10.

Figure S5

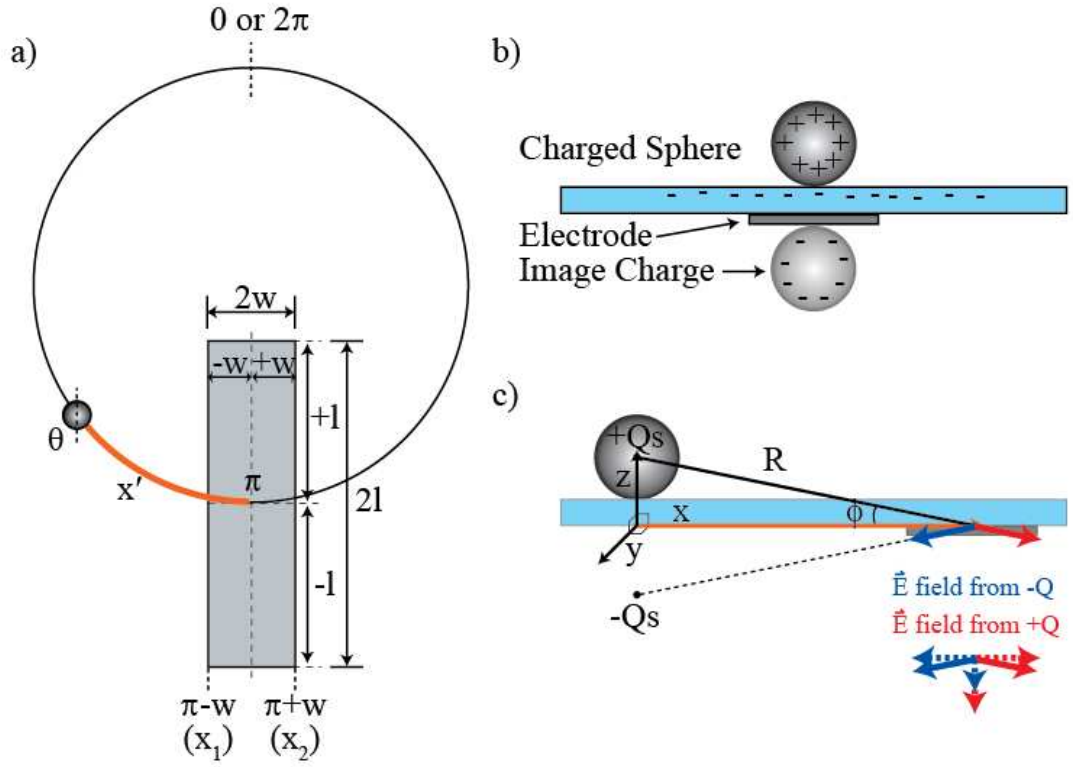

We assumed that the difference between x□ and x was negligible.

$$\vec{E} = \frac{Q}{4\pi\varepsilon_o R^2}$$

$$R^2 = z^2 + x^2 + y^2$$

$$R = \sqrt{z^2 + x^2 + y^2}$$

$$\vec{E} = \frac{Q}{4\pi\varepsilon_o \left(z^2 + x^2 + y^2\right)}$$

Since: $\sin\phi = \frac{z}{R}$

z component of $\vec{E}$

$$\vec{E}_z = \vec{E}\sin\phi = \frac{Qz}{4\pi\varepsilon_o R^3} = \frac{Qz}{4\pi\varepsilon_o \left(z^2 + x^2 + y^2\right)^{3/2}}$$

Since there are 2 z components (one from the real charge and one from the image charge):

$$\vec{E}_{tot} = \vec{E}_z - (-\vec{E}_z) = 2\vec{E}\sin\phi = \frac{Qz}{2\pi\varepsilon_o\left(z^2 + x^2 + y^2\right)^{3/2}}$$

$Q_e = \int A_{electrode}\left(\varepsilon_o \vec{E} dydx\right)$, A is the surface area of the electrode

$$Q_e = \varepsilon_o \int_{x_1}^{x_2}\int_{y_1}^{y_2} \vec{E}_{tot} dydx$$

Here the limits y_1 and y_2 are $-l$ and $+l$, and x_1 and x_2 are (π-w-θ) and (π+w-θ)

$$Q_e = \frac{Q_s z}{2\pi}\int_{\pi-w-\theta}^{\pi+w-\theta}\int_{-l}^{+l}\frac{1}{\left(z^2 + x^2 + y^2\right)^{3/2}} dydx$$

By symmetry $-l$ to $+l$ is $2l$:

$$Q_e = \frac{Q_s z}{\pi}\int_{\pi-w-\theta}^{\pi+w-\theta}\int_{0}^{+l}\frac{1}{\left(z^2 + x^2 + y^2\right)^{3/2}} dydx$$

Integrate over y:

$$\int_0^{+l}\frac{1}{\left(z^2 + x^2 + y^2\right)^{3/2}} dy$$

$$= \frac{Q_s z}{\pi\left(x^2 + z^2\right)}\left(\frac{y}{\sqrt{y^2 + x^2 + z^2}}\right)\Big|_0^l$$

$$= \frac{Q_s z}{\pi\left(x^2 + z^2\right)}\left(\frac{l}{\sqrt{l^2 + x^2 + z^2}}\right)$$

Since: $l >> x^2 + z^2$,

Therefore: $$Q_e = \frac{Q_s z}{\pi}\int_{\pi-w-\theta}^{\pi+w-\theta}\frac{1}{\left(x^2 + z^2\right)} dx$$

Integrate over x:

$$Q_e = \frac{Q_s}{\pi}\left[\arctan\left(\frac{x}{z}\right)\right]\Big|_{\pi-w-\theta}^{\pi+w-\theta}$$

$$= \frac{Q_s}{\pi}\left[\arctan\left(\frac{\pi+w-\theta}{z}\right) - \arctan\left(\frac{\pi-w-\theta}{z}\right)\right]$$

$$= \frac{Q_s}{\pi}\left[\arctan\left[-\left(\frac{\theta-\pi-w}{z}\right)\right]\right] - \left[\arctan\left[-\left(\frac{\theta-\pi+w}{z}\right)\right]\right]$$

$$= \frac{Q_s}{\pi}\left[\arctan\left(\frac{\theta-\pi+w}{z}\right) - \arctan\left(\frac{\theta-\pi-w}{z}\right)\right]$$